

DA-MUSIC: Data-Driven DoA Estimation via Deep Augmented MUSIC Algorithm

Julian P. Merkofer, *Student Member, IEEE*, Guy Revach, *Student Member, IEEE*, Nir Shlezinger, *Member, IEEE*, Tirza Routtenberg, *Senior Member, IEEE*, and Ruud J. G. van Sloun, *Member, IEEE*

Abstract—Direction of arrival (DoA) estimation of multiple signals is pivotal in sensor array signal processing. A popular multi-signal DoA estimation method is the multiple signal classification (MUSIC) algorithm, which enables high-performance super-resolution DoA recovery while being highly applicable in practice. MUSIC is a model-based algorithm, relying on an accurate mathematical description of the relationship between the signals and the measurements and assumptions on the signals themselves (non-coherent, narrowband sources). As such, it is sensitive to model imperfections. In this work we propose to overcome these limitations of MUSIC by augmenting the algorithm with specifically designed neural architectures. Our proposed deep augmented MUSIC (DA-MUSIC) algorithm is thus a hybrid model-based/data-driven DoA estimator, which leverages data to improve performance and robustness while preserving the interpretable flow of the classic method. DA-MUSIC is shown to learn to overcome limitations of the purely model-based method, such as its inability to successfully localize coherent sources as well as estimate the number of coherent signal sources present. We further demonstrate the superior resolution of the DA-MUSIC algorithm in synthetic narrowband and broadband scenarios as well as with real-world data of DoA estimation from seismic signals.

I. INTRODUCTION

Source separation, localization, and tracking are crucial tasks in sensor array processing. In particular, direction of arrival (DoA) estimation of multiple, broadband, and possibly coherent signal sources plays a key role in a wide range of applications, including radar, communications, image analysis, and speech enhancement [2], [3], [4]. Over the last decades, a multitude of different DoA estimation algorithms have been proposed, and the problem is an active area of research [5], [6].

A leading scheme employed in many DoA applications is the popular multiple signal classification (MUSIC) algorithm [7], which can provide asymptotically unbiased estimates of the number of incident wavefronts present, their approximate frequencies, and their DoAs. MUSIC and other classic approaches, e.g., conventional beamforming [8] and MVDR beamforming [9], are based on knowledge of the underlying statistical model; this dependency induces several key limitations. Among the drawbacks of the model-based (MB) approaches is the inherent limitation of the signal model from which they are

derived, which considers narrowband signals. This results, for example, in the inability to consistently estimate the DoA of correlated (coherent) signals, as well as a failure to resolve closely spaced signals with an insufficient number of samples or a low signal-to-noise ratio (SNR) [7], [5].

To extend narrowband models to broadband DoA estimation, various extensions and alternative approaches have been explored [10], because when the impinging signals are broadband, multiple frequency ranges can carry different information regarding the DoA angles at hand. Generally, these extensions from narrowband to broadband can be subdivided into coherent and incoherent processing methods. In coherent methods, the covariance matrices of the observations in different frequency bins are coherently combined using certain transformation matrices. Most coherent techniques are based on the coherent signal subspace (CSS) concept [11], which focuses the transformations of the covariances at different frequencies into a surrogate narrowband model, yet utilizes different transformation matrices. Incoherent broadband processing methods combine DoA estimates obtained separately for each frequency bin [12].

The recent success of data-driven (DD) deep learning across a wide range of disciplines gave rise to neural network (NN)-aided DoA estimators. The works [13], [14], [15] implemented model-agnostic DoA estimation using a dense NN, a convolutional NN (CNN), and a U-Net architecture, respectively. While such black-box NNs enable handling array imperfections due to their model-agnostic nature, they involve highly parameterized models that may be computationally intensive and lack the interpretability of MB methods. Alternatively, NNs were used to robustify the MB MUSIC as a form of hybrid MB/DD system [16], [17]. Specifically, the work [18] proposed to estimate the discretized MUSIC spectrum from the covariance matrix of the measurements through the utilization of multiple convolutional NNs. While this method is more robust to model inaccuracies compared with the original MUSIC algorithm, utilizing the MUSIC spectrum as a label for training causes it to experience the same drawbacks as its MB counterpart. Another DD approach proposed in [19] considered systems with subarray sampling and uses NNs to obtain a single estimated covariance matrix from incoherent subarray measurements. This NN-aided estimate is utilized for DoA recovery via the subspace-based MUSIC algorithm. The method addresses the fundamental dependency of MUSIC on the estimated covariance matrix, thereby robustifying the MUSIC algorithm, yet it does not fully exploit the NNs' ability to improve MUSIC, as the NN is trained using the true covariance matrix as a label, without considering its downstream task.

Parts of this work were presented in the 2022 IEEE International Conference on Acoustics, Speech, and Signal Processing (ICASSP) as the paper [1]. J. P. Merkofer is with the EE Dpt., Eindhoven University of Technology, Eindhoven, The Netherlands (e-mail: j.p.merkofer@tue.nl), this work was partially done while being with the ETH Zürich. G. Revach is with the D-ITET, ETH Zürich, Switzerland, (email: grevach@ethz.ch). N. Shlezinger and T. Routtenberg are with the School of ECE, Ben-Gurion University of the Negev, Beer Sheva, Israel (e-mail: {nirshl; tirzar}@bgu.ac.il). R. J. G. van Sloun is with the EE Dpt., Eindhoven University of Technology, and with Phillips Research, Eindhoven, The Netherlands (e-mail: r.j.g.v.sloun@tue.nl).

The works [20], [21] applied CNNs for broadband DoA estimation of a single source. The two approaches, however, utilize very different preprocessing methods and are trained as classification and regression tasks, respectively. While the classification approach limits itself to a fixed resolution, the regressor of [21] outputs the DoA angles directly. Therefore, it can achieve an arbitrary resolution, yet it is limited to the spatial covariance matrix as input.

These limitations of both existing MB and DD DoA estimation algorithms in resolving multiple signals that are possibly broadband and coherent motivates the derivation of a NN-aided DoA estimator capable of leveraging data to enable MUSIC to successfully operate in such scenarios.

In this work we propose DA-MUSIC [1], a hybrid MB/DD implementation of MUSIC, which exploits the structure of the classic MUSIC algorithm while augmenting it with NNs to learn to enhance its performance. The proposed architecture overcomes the fundamental limitations of MUSIC, enabling it to successfully estimate the number of signal sources present as well as accurately detect their locations for coherent sources in narrowband as well as broadband scenarios. Our design builds upon the insight that the sensitivity to model mismatch and inability to handle coherent and broadband sources of MUSIC lie in its estimation of the noise and signal subspaces through an eigenvalue decomposition (EVD) of the empirical covariance matrix. Accordingly, the proposed DA-MUSIC improves this crucial step by obtaining a surrogate, pseudo covariance matrix through a recurrent NN (RNN) from the measurements, which is learned along with a NN that acts as a peak finder.

Our experimental study demonstrates the ability of the proposed architecture to notably improve upon both MB and DD DoA estimators. In particular, we show that the DA-MUSIC algorithm outperforms its unaltered version in localization accuracy and resolution for both synthetic settings, as well as for DoA estimation from measurements of complex broadband seismic signals.

The rest of the paper is organized as follows: Section II describes the assumed system model and surveys some of the related work of DoA estimation, as well as the technical details of the MB MUSIC algorithm; Section III introduces the DA-MUSIC algorithm; Section IV presents the results of the simulations; and Section V provides concluding remarks.

Throughout the paper, we use boldface lower-case letters for vectors; e.g., \mathbf{x} , and boldface upper-case letters, e.g., for \mathbf{X} . The i th entry of a vector \mathbf{x} is denoted by x_i . We use calligraphic letters to denote the discrete-time Fourier transform, e.g., $\mathcal{X}(\omega)$ is the frequency representation of a signal $x(t)$. We use $(\cdot)^\top$ and $(\cdot)^H$ to denote the transpose and Hermitian operators respectively, and $\|\cdot\|$ and $\|\cdot\|_F$ to denote the ℓ_2 and Forbenius norms respectively. Further, \mathcal{U} and \mathcal{CN} represent the uniform and the complex normal distributions. The symbol \mathbb{I} denotes the identity matrix.

II. SYSTEM MODEL AND PRELIMINARIES

In this section we detail the system model for which we develop the proposed DA-MUSIC algorithm in Section III. To that aim, we first discuss the signal model in Subsection II-A. Then,

we formulate the DoA estimation problem in Subsection II-B, and survey some of the related literature in Subsection II-C. Since our proposed solution builds upon the MUSIC algorithm, we recall MUSIC in Subsection II-D and briefly discuss the CSS method for broadband extension in Subsection II-E.

A. Signal Model

We distinguish the considered signal model into two cases: the conventional narrowband settings, and its more general broadband setup. For more details regarding the two models, we refer the reader to the textbooks [22], [10], and [23].

1) *Narrowband*: The most common setup in the array signal processing literature concerning DoA estimation is the narrowband setting. Here, the time it takes for the waves to propagate the array is assumed to be negligible such that the occurring delays are sufficiently small. Therefore, the signal measurement model for an arbitrary array structure consisting of M sensor elements measuring D impinging narrowband signals takes the following form:

$$\mathbf{x}(t) = \mathbf{A}(\boldsymbol{\theta}) \mathbf{s}(t) + \mathbf{v}(t). \quad (1)$$

In (1), the measurements $\mathbf{x}(t) \in \mathbb{C}^M$ at time instance t depend on the signals $\mathbf{s}(t) \in \mathbb{C}^D$, which originate from the unknown angles $\boldsymbol{\theta} = [\theta_1, \dots, \theta_D]$, while $\mathbf{v}(t) \in \mathbb{C}^M$ is additive white Gaussian noise. The matrix $\mathbf{A}(\boldsymbol{\theta}) \in \mathbb{C}^{M \times D}$ contains the steering vectors $\{\mathbf{a}(\theta_d)\}$, i.e.,

$$\mathbf{A}(\boldsymbol{\theta}) = [\mathbf{a}(\theta_1) \dots \mathbf{a}(\theta_D)], \quad (2)$$

where $\{\theta_d\}$ are the source directions. For example, the steering vector $\mathbf{a}(\psi)$ for a uniform linear array (ULA) with an element spacing of $\Delta m = \ell/2$, where ℓ is the wavelength of the signals, is defined for direction ψ as

$$\mathbf{a}(\psi) = [1 \ e^{-j\pi \sin \psi} \ \dots \ e^{-j\pi(M-1) \sin \psi}]. \quad (3)$$

Consequently, the steering vectors (and, in turn, the matrix $\mathbf{A}(\boldsymbol{\theta})$) specify the underlying array geometry. The collection of the measurements at the array elements over multiple time instances is defined as

$$\mathbf{X} = [\mathbf{x}(1) \ \dots \ \mathbf{x}(T)], \quad (4)$$

where T is referred to as the number of snapshots.

2) *Broadband*: In practice, many signals are broadband, and the delay caused by propagating the array aperture needs to be incorporated in the signal model. The following notation models the measurements received at array element $m \in \{1, \dots, M\}$

$$x_m(t) = \sum_{d=1}^D s_d(t - \tau_{md}) + v_m(t), \quad (5)$$

where τ_{md} represents the time delay of the m th array element measuring source $d \in \{1, \dots, D\}$ compared to the measurement at the reference element $m = 1$. Transformed to the frequency domain, the relationship in (5) at frequency ω becomes

$$\mathcal{X}_m(\omega) = \sum_{d=1}^D e^{-j\omega\tau_{md}} \mathcal{S}_d(\omega) + \mathcal{V}_m(\omega), \quad (6)$$

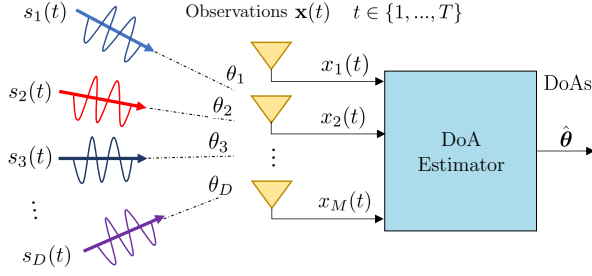


Fig. 1: DoA estimation illustration.

which can in turn be written in vector-matrix form analogous to the narrowband system model (1) as follows:

$$\mathcal{X}(\omega) = \mathbf{A}(\omega, \theta) \mathcal{S}(\omega) + \mathcal{V}(\omega). \quad (7)$$

For a ULA, the broadband steering vectors are defined for frequency ω and angle of interest ψ as

$$\mathbf{a}(\omega, \psi) = [1 \ e^{-j\omega \frac{\Delta m}{c} \sin \psi} \ \dots \ e^{-j\omega(M-1) \frac{\Delta m}{c} \sin \psi}], \quad (8)$$

where c is the propagation velocity.

B. Problem Formulation

DoA estimation is concerned with localizing signal sources by determining their angles of incidence utilizing the measurements of an array aperture [22]. Formally, this corresponds to estimating the angles $\theta = [\theta_1 \dots \theta_D]$ from the measurements $\mathbf{x}(t) = [x_1(t) \dots x_M(t)]^T$ measured at multiple time instances $t \in \{1, \dots, T\}$. An illustration of such a system is depicted in Fig. 1. The following additional assumptions are imposed upon the observation model as well as the derived synthetic data. The signals are uncorrelated to the noise (though signals may possibly be correlated with each other) and generated in the far-field region. And there is uniform propagation in all directions in an isotropic and non-dispersive medium. We further assume that we have knowledge (though possibly mismatched) of the underlying array geometry, implying that we can compute an approximation of $\mathbf{a}(\psi)$ or $\mathbf{a}(\omega, \psi)$. We consider a data-driven setting where we have access to training data. This data is a set of U pairs, $\{(\mathbf{X}_u, \theta_u)\}_{u=1}^U$, each comprising the observations and DoA angles from where the signals originated. In many scenarios; e.g., in wireless communications, a specific training set can be developed before deployment. If the ground-truth DoAs are not obtainable at all, the data-driven DoA estimator must be trained by utilizing synthetic data that closely describes the real signals. Our goal is thus to leverage the available domain knowledge and data to design a system for recovering the DoAs θ from a corresponding observation matrix \mathbf{X} whose columns are T snapshots of the measured waveforms at the M sensors.

C. Related Literature

We next provide an overview of relevant DoA estimation methods based on the above problem formulation, motivating the need for our proposed DA-MUSIC detailed in Section III. An extensive overview of various MB DoA estimators can

be found in [5], [6], and a recent literature review of DD DoA estimation approaches can be found in [24]. We thus only discuss some representative MB methods, followed by reviewing relevant broadband extensions, and conclude with DD architectures for narrowband as well as broadband signals.

1) *MB Narrowband Estimators*: The conventional beamformer (i.e. maximizing the steered response) is a basic approach to DoA estimation and an extension of classical Fourier-based spectral analysis [8]. Various improvements and alternative beamforming methods have been developed, such as the minimum variance distortionless response beamformer [9] and other adaptive beamformers [25]. An overview of beamforming techniques can be found in [26].

An alternative family of DoA estimators is based on subspace methods, which aim at recovering the DoAs by identifying the noise and signal subspaces. The MUSIC algorithm [7] is a highly popular subspace-based method and has been researched extensively. Being the focus of this paper, more information and a detailed description of the algorithm can be found in Section II-D. Extensions of MUSIC include Root-MUSIC [27], a polynomial-rooting version, as well as spatially smoothed MUSIC, which removes the correlation between the incident signals by dividing the receiver array into overlapping subarrays [28]. In practice, however, the number of coherent sources is mostly unknown, and therefore the decorrelation effect of spatial smoothing is not obvious [29]. Another popular subspace-based method for DoA estimation is estimation of signal parameters via rotational invariance techniques (ESPRIT) [30] and its variations [31]. These methods rely heavily on the accuracy of the underlying model assumptions, are generally sensitive to array aperture perturbations, and are inherently derived for narrowband signals.

2) *MB Broadband Estimators*: Broadband DoA estimation algorithms can be categorized into two groups: incoherent methods and coherent methods. Generally, incoherent methods use independent frequency bins (IFBs) to process the DoA information at every frequency separately and then combine the results of these narrowband DoA estimations. There are many different variations in the implementation of this approach [32], [33], [34], which typically vary in the computation of the covariance matrices. Unfortunately, the computational complexity increases with each frequency bin.

Conversely, coherent methods combine the covariance matrices estimated for IFBs in order to apply narrowband techniques directly over a single, so-called focused covariance matrix. An overview of coherent techniques can be found in [10], [35]. A leading approach for coherent broadband DoA estimation is based on the CSS method [11], with example estimators given in [36], [37], [38]. Many variations of the CSS method are concerned with the crucial aspect of the focusing strategy, proposing different techniques to combine the covariances at each IFB to obtain a faithful narrowband formulation. See, for example, [39], [40] and the more recent summary [41]. These methods, however, experience significant bias with larger angular sectors of interest and can impose additional model assumptions such as noise statistics.

3) *DD Estimators*: Inspired by the dramatic success of deep learning in computer vision and natural language processing,

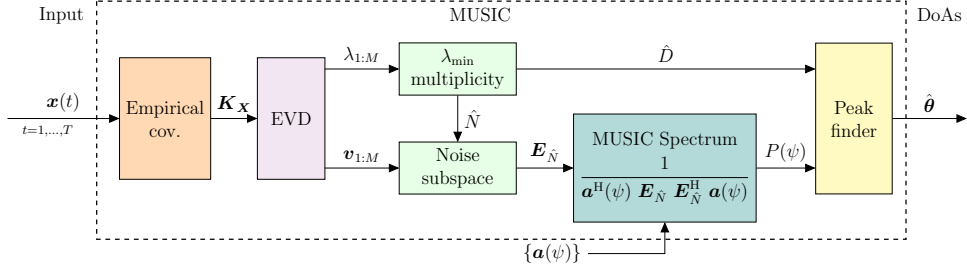


Fig. 2: Block diagram of the MUSIC algorithm.

recent years have witnessed a growing interest in the application of NNs for DD DoA estimation. The works [13], [14] implement DoA estimation algorithms in a black-box manner using dense and convolutional NNs, respectively. The work [15] trained a U-Net model to segment a discretized angle grid for identifying multiple DoAs. While these purely DD approaches rely less on the accuracy of the assumed data model, they require highly parameterized NNs that often lack generalization and interpretability, and are computationally intensive.

Alternatively, hybrid MB/DD systems are implemented in [18] and [19]. Specifically, [18] proposed to estimate the discretized MUSIC spectrum from the covariance matrix of the measurements through the utilization of multiple convolutional NNs. However, utilizing the MB MUSIC spectra as training labels limits the approach to the same drawbacks of its MB counterpart. The work [19] considers systems with subarray sampling and uses NNs to obtain a single estimated covariance matrix from incoherent subarray measurements. This NN-aided estimate is then utilized for DoA recovery via the classic MUSIC algorithm. The method addresses the fundamental dependency of MUSIC on the estimated covariance matrix; yet again, training using the true covariance matrix as a label does not fully exploit the capability of the NNs.

The works [20] and [21] both propose a CNN architecture for broadband DoA estimation of one single source. The two approaches, however, utilize very different preprocessing methods and are trained as classification and regression tasks, respectively. The classification CNN outputs the posterior probabilities of the DoA classes from the phase component of each frequency bin generated by the fast Fourier transform (FFT) of the measurements, thereby limiting itself to a fixed resolution. While the regressor can achieve an arbitrary resolution, it limits itself to the spatial covariance matrix as input and to the resulting information loss when the measurements are correlated.

D. MUSIC Algorithm

As our proposed DA-MUSIC algorithm originates from the MUSIC algorithm, we next present this method in detail. MUSIC, originally proposed by Schmidt in [7], considers the narrowband signal model with incoherent sources (1), where the signals in $\mathbf{s}(t)$ are mutually independent. Fig. 2 visualizes a simple outline of the MUSIC structure as a block diagram. The approach takes the empirical covariance matrix of the received measurements \mathbf{X} , then conducts an EVD,

followed by categorizing the eigenvectors into signal and noise subspaces. The orthogonality between the two subspaces allows the formulation of a spatial spectrum, which contains peaks at DoA angles.

1) *Formal Derivation:* With the assumption of the signal and the noise being uncorrelated, the covariance matrix of $\mathbf{x}(t)$ is given by

$$\mathbf{K}_{\mathbf{X}} = \mathbf{A}(\boldsymbol{\theta})\mathbf{K}_{\mathbf{S}}\mathbf{A}^H(\boldsymbol{\theta}) + \lambda\mathbf{K}_{\mathbf{X}}^0, \quad (9)$$

with $\mathbf{K}_{\mathbf{S}}$ being the covariance of the incident signals $\mathbf{s}(t)$. The matrix $\mathbf{A}(\boldsymbol{\theta})\mathbf{K}_{\mathbf{S}}\mathbf{A}^H(\boldsymbol{\theta})$ is singular and has a rank of less than M when the number of array elements M is strictly larger than the number of signals D . Therefore, λ is an eigenvalue of $\mathbf{K}_{\mathbf{X}}$ (in the metric of $\mathbf{K}_{\mathbf{X}}^0$, which takes the form $\mathbf{K}_{\mathbf{X}}^0 = \sigma^2\mathbf{I}$ for additive white Gaussian noise (AWGN) with variance σ^2). Further, $\mathbf{A}(\boldsymbol{\theta})\mathbf{K}_{\mathbf{S}}\mathbf{A}^H(\boldsymbol{\theta})$ has to be non-negative definite, because $\mathbf{A}(\boldsymbol{\theta})$ has full rank and $\mathbf{K}_{\mathbf{S}}$ is positive definite, and consequently, λ in (9) is the minimal eigenvalue of $\mathbf{K}_{\mathbf{X}}$, denoted λ_{\min} . The multiplicity of λ_{\min} corresponds to the number of incident wavefronts, and equals $N = M - D$.

MUSIC builds upon this representation of the covariance of the signals. The algorithm takes as input T snapshots of the waveforms at M array elements, represented as \mathbf{X} in (4), and uses them to obtain an empirical estimate of $\mathbf{K}_{\mathbf{X}}$ via $\hat{\mathbf{K}}_{\mathbf{X}} = \frac{1}{T}\mathbf{X}\mathbf{X}^H$. Then, the number of incident signals D is estimated via

$$\hat{D} = M - \hat{N}, \quad (10)$$

where \hat{N} is the estimated multiplicity of the minimal eigenvalue of $\hat{\mathbf{K}}_{\mathbf{X}}$. The eigenvectors corresponding to the \hat{N} smallest eigenvalues form the noise subspace $\mathbf{E}_{\hat{N}}$, which is orthogonal to the D dimensional signal subspace spanned by the incident signal mode vectors. Consequently, MUSIC estimates the DoAs by computing the spatial spectrum

$$P(\psi) = \frac{1}{\mathbf{a}^H(\psi)\mathbf{E}_{\hat{N}}\mathbf{E}_{\hat{N}}^H\mathbf{a}(\psi)}, \quad (11)$$

and the \hat{D} dominant peaks of $P(\psi)$ are set as the estimated DoA angles $\hat{\boldsymbol{\theta}}$.

MUSIC is a popular and highly applicable subspace-based method that is reasonably efficient and statistically consistent [42], [5]. When the signal model is adequately accurate, it can achieve super-resolution and deliver a highly accurate estimate of the number of signal sources present. Nevertheless, the algorithm is sensitive towards the accuracy of the empirical estimate of $\mathbf{K}_{\mathbf{X}}$, and cannot reliably estimate the DoA angles

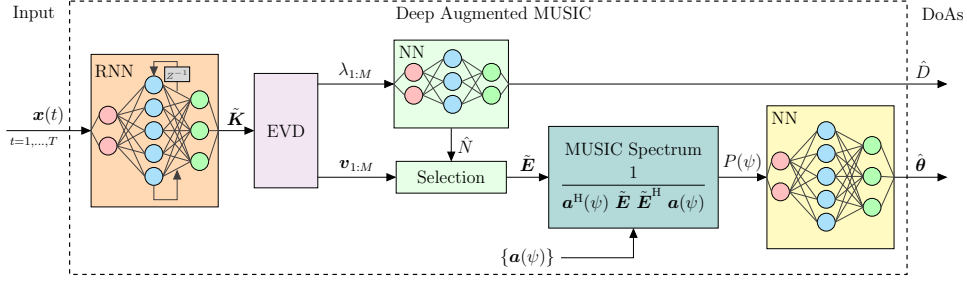


Fig. 3: Block diagram of the DA-MUSIC algorithm.

as well as the number of sources of coherent signals. The reason for this is that highly correlated signals cause zero entries within the covariance matrix and can, therefore, become indistinguishable from noise [43]. Furthermore, the MUSIC algorithm is inherently a narrowband approach due to the assumptions imposed on the system model. Nonetheless, it can be extended to broadband, i.e., signal models as in (7), and so we next describe the coherent method to achieve this, which is also adopted in our proposed DA-MUSIC.

E. Coherent Broadband

The main concept behind coherent broadband DoA estimation is to transform the different frequency covariance matrices into a single covariance matrix at a focusing frequency. Accordingly, coherent methods find appropriate transformations for each frequency, transform the covariances, and obtain a focused covariance matrix by some form of averaging. In particular, the CSS method [11] aims at combining the spatial signal subspaces to align the signal subspaces associated with the DoA along all frequency bins. To formulate this, let $\mathbf{K}(\omega)$ be the covariance of the frequency domain observations (7), and divide the spectrum into B IFBs with central frequencies $\{\omega_b\}_{b=1}^B$. The focused covariance matrix, which is used as the input covariance for narrowband DoA recovery, is estimated as

$$\mathbf{K} = \sum_{b=1}^B \alpha_b \mathbf{T}_b \mathbf{K}(\omega_b) \mathbf{T}_b^H, \quad (12)$$

where α_b is a weighting and \mathbf{T}_b is the focusing matrix. The focusing matrices can be determined by attempting to focus the spectral components at some frequency ω_r and some focusing angles ψ by solving

$$\mathbf{T}_b = \arg \min_{\mathbf{T}} \|\mathbf{A}(\omega_r, \psi) - \mathbf{T} \mathbf{A}(\omega_b, \psi)\|_F. \quad (13)$$

Coherent techniques have been shown to achieve a better estimation accuracy and a smaller computational complexity as well as a lower resolution threshold than non-coherent methods [41]. However, the CSS methods require initial values for the focusing matrix \mathbf{T} , the reference frequency ω_r , and the relevant focusing angles ψ to find the focusing matrices with (13), and are typically sensitive towards these initial values. Additionally, it is not guaranteed that the alignment of the signal and noise subspaces exists to form a viable general covariance matrix without disarranging the noise subspace [40].

III. DEEP AUGMENTED MUSIC

DA-MUSIC is a hybrid MB/DD DoA estimation algorithm derived from the classic MUSIC algorithm by replacing crucial and model mismatch sensitive elements of the model-based structure with specific NNs. Fig. 3 outlines the resulting structure of the DA-MUSIC architecture and highlights the remaining similarities to the original MUSIC algorithm, depicted in Fig. 2.

Principally, DA-MUSIC builds upon the understanding that the core challenges associated with the classic MUSIC algorithm can be tackled by providing a surrogate covariance matrix. In particular, as the CSS method provides a surrogate covariance \mathbf{K} that transforms a broadband signal model into a narrowband one, a similar approach can be employed to handle coherent sources and array mismatches. Therefore, to improve the categorization of the noise and signal subspaces, the correlation of the received measurements is learned from temporal data by employing a dedicated RNN, which is augmented into the overall flow of MUSIC. We next elaborate on the architecture in Subsection III-A, after which we present the training method in Subsection III-B and provide a discussion in Subsection III-C.

A. Architecture

The proposed DA-MUSIC algorithm preserves the structure of the MB MUSIC while replacing certain critical aspects with NNs. Our neural augmentations aim to improve the crucial steps of estimating the noise and signal subspaces from the empirical covariance and the translation of the spatial spectrum into DoAs via peak finding. By doing so, DA-MUSIC is not constrained by the additional model assumptions imposed in the derivation of MUSIC, and can, as we will show, e.g. learn to successfully localize coherent signals. To present the architecture of DA-MUSIC, we commence with the simple case where the number of sources D is known, and then show how its estimation is incorporated. Details of the NNs used in our experimental study are reported in Section IV.

1) *Known Number of Sources:* Fig. 4 depicts a detailed outline of the individual elements of the DA-MUSIC architecture. The respective output dimensions of the corresponding components are given in the bracket notation. First, the input signal $\mathbf{x}(t)$ is transformed into the pseudo covariance matrix $\tilde{\mathbf{K}}$ using a RNN implemented through a gated recurrent unit (GRU). The final state of the GRU is passed to a dense layer enabling a reshaping to the desired dimension of the pseudo

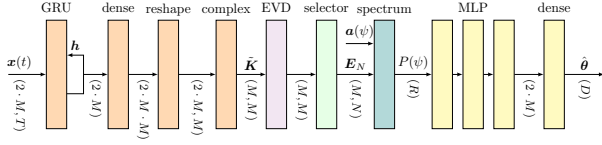


Fig. 4: Detailed network structure of the DA-MUSIC algorithm.

covariance matrix $\hat{\mathbf{K}}$ as well as the subsequent transformation of the complex space. Then, through the continued use of the EVD, the algorithm categorizes the subspaces using the eigenvectors. Inserting the steering vectors $\mathbf{a}(\psi)$ allows to compute an estimate of the spatial spectrum in (11), denoted $P(\psi)$, identically to MB MUSIC, by using the noise eigenvectors selected from $\hat{\mathbf{K}}$.

Next, DA-MUSIC attains the DoAs from the spatial spectrum $P(\psi)$ using an additional NN, comprised of a multi-layer perceptron (MLP) of three fully connected dense layers followed by a single dense layer with linear activation. The input to the MLP are R samples of $P(\psi)$ taken uniformly in $[0, 2\pi)$. The output of the MLP is the set of estimated DoA angles $\hat{\theta}$. The benefits of using a NN-based peak-finder compared to a model-based one are two-fold. First, learning the translation of the pseudo-spectrum into DoAs from data enables achieving improved resolution compared to conventional peak finding, since $\hat{\theta}_d \in [0, 2\pi)$ instead of being dependent on the number of angles ψ used to evaluate the spectrum. Furthermore, peak finding is generally non-differentiable; thus, replacing it with a NN facilitates training DA-MUSIC end-to-end. The resulting architecture enables the application of gradient-based optimization, by propagating through the NNs as well as the EVD operation, as done in [44]. Doing so allows to jointly tune the noise subspace recovery along with the translation of the MUSIC spectrum into DoAs by comparing its estimated DoAs with the true DoAs, as we detail in Subsection III-B.

2) *Varying Number of Sources*: Delivering unbiased estimates of the number of signal sources as well as the ability to successfully localize these sources makes MUSIC highly applicable. The above discussed DA-MUSIC architecture can be extended to operate with a potentially unknown and varying number of signal sources, despite the determinant nature of the NNs. This is achieved by addressing three key aspects of the algorithm: the estimation of the number of sources; the selection process of the noise subspace from the eigenvectors; and the adaptation of the output strategy to overcome the varying number of DoA angles.

Estimating number of sources: Our design allows DA-MUSIC to learn abstract mappings as pseudo covariance features $\hat{\mathbf{K}}$, which is geared towards end-to-end training and is not restricted to a natural ordering of the model-based covariances. Consequently, instead of estimating the number of sources by inspecting the magnitude of its eigenvalues, we opt a data-driven approach. We augment the process of estimating the number of sources with a classifier, implemented through a MLP, as a classification task. Since subspace methods with M inputs can resolve at most $M - 1$ signals, the classifier has $M - 1$ classes. Fig. 5 depicts the DA-MUSIC architecture with an added classifier taking the eigenvalues as an input and

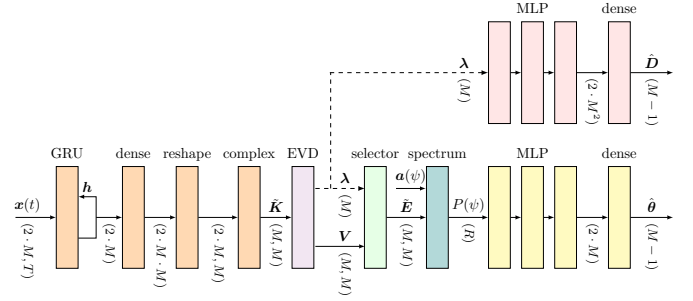


Fig. 5: DA-MUSIC algorithm with a separately trained (internal) classifier.

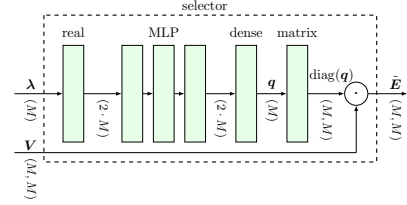


Fig. 6: Detailed outline of the DA-MUSIC subspace selection augmentation.

outputting an estimate of the number of sources.

Computing noise subspace: The noise subspace selector needs to know the number of sources $D \in \{1, \dots, M - 1\}$ to classify the eigenvectors into signal and noise subspaces; i.e., by choosing the eigenvectors corresponding to the $N = M - D$ smallest eigenvalues. When the number of sources is not known, we propose to weight each eigenvector by an estimate of it belonging to the noise subspace. We do this by introducing an additional neural augmentation, depicted in Fig. 6, which uses a MLP to cluster the eigenvalues in a learned fashion.

In particular, the MLP maps the estimated M eigenvalues into a vector $\mathbf{q} = [q_1, \dots, q_M]$ whose entries hold the individual probabilities of choosing the corresponding eigenvector as a noise eigenvector. The selection is performed by computing $\hat{\mathbf{E}} = \mathbf{V} \text{diag}(\mathbf{q}) = [q_1 \mathbf{v}_1 \dots q_M \mathbf{v}_M]$, allowing to learn a suitable noise subspace. Note that this setting specializes into the conventional approach of assigning based on the multiplicity of the minimal eigenvalues; in the conventional approach, the entries of \mathbf{q} are either ones or zeros, and $\hat{\mathbf{E}}$ coincides with the corresponding subspace. Consequently, the proposed approach provides additional flexibility in selecting the noise subspace and facilitates coping with settings where distinguishing between the eigenvectors is challenging due, for example, to low SNRs.

Outputting varying number of DoAs: The most common strategy to overcome the dynamic output dimensions of NNs is to scale the output dimension to the maximum occurring value. In our case, since MUSIC cannot resolve more than $M - 1$ sources, the dimension of the last dense layer of DA-MUSIC is set to $M - 1$. The only additional modification required with this strategy compared with known D is the slight alteration to the loss function discussed in Subsection III-B below. An advantage of this strategy is that the approach allows to extract up to $M - 1$ DoA, where θ_1 is most likely a true DoA angle,

θ_2 has a slightly lower probability to be a DoA angle, etc. The final estimation is thus carried out by first taking \hat{D} from the module that estimates the number of sources, and then using the first \hat{D} outputs as the recovered DoAs.

B. Training Procedure

DA-MUSIC is trained end-to-end in a supervised setting as a multiple regression problem. As detailed in Subsection II-B, the training set is comprised of U tuples of sequences of measurements and their corresponding DoAs; i.e., the u^{th} tuples includes the T_u measurements \mathbf{X}_u and their corresponding D_u DoA angles θ_u . We first describe how this data is used for training when D is known and fixed; i.e., $D_u \equiv D$. This acts as a preliminary step for discussing how the training procedure is carried out in the general case where the model does not have knowledge D .

1) *Known Number of Sources*: Given a sequence of measurements \mathbf{X} as input, the model predicts the estimated DoA angles $\hat{\theta}$ that are compared to the true DoA angles θ . Gradient-based optimization is possible because every element of the architecture is differentiable, allowing backpropagation through the complete structure. Derived from the root mean squared periodic error (RMSPE) [45], [46] the following loss function additionally compares all permutations of the predicted angles with the true angles to capture all possible assignments of the estimated DoA to the true DoA. Thereby the minimal permutation RMSPE includes the permutation invariance of the DoAs and is obtained as:

$$\text{RMSPE}(\theta, \hat{\theta}) = \min_{\mathbf{P} \in \mathcal{P}_D} \left(\frac{1}{D} \left\| \text{mod}_{\beta}(\theta - \mathbf{P}\hat{\theta}) \right\|^2 \right)^{\frac{1}{2}}, \quad (14)$$

where \mathcal{P}_D is the set of all $D \times D$ permutations and mod_{β} denotes the element-wise modulus operation regarding the angle range of interest, e.g. $\beta = \pi$ for $\psi \in [-\pi/2, \pi/2)$ or $\beta = 2\pi$ for $\psi \in [0, 2\pi)$.

2) *Unknown Number of Sources*: As discussed in the previous subsection, DA-MUSIC is designed to resolve a varying and unknown number of sources by introducing an additional NN classifier for the number of sources. To formulate the training procedure of the overall system, we use \mathbf{w}_c to denote the trainable parameters of the classifier, while \mathbf{w}_d represents the parameters of the remaining trainable modules of DA-MUSIC (covariance estimator, peak finder, and subspace selector). The loss used to train \mathbf{w}_d is the RMSPE loss of (14), which is altered during training to account for varying sources by computing,

$$\mathcal{L}_{\text{RMSPE}}(\theta_u, \hat{\theta}(\mathbf{X}_u)) = \text{RMSPE}(\theta_{1:D_u}, \hat{\theta}_{1:D_u}(\mathbf{X}_u)). \quad (15)$$

In (15), $\hat{\theta}(\mathbf{X}_u)$ denotes the $M - 1$ outputs of DA-MUSIC applied to \mathbf{X}_u , while $\theta_{1:D_u} = (\theta_1, \dots, \theta_{D_u})$. This means that only the first D_u angles of the estimated DoA $\hat{\theta}$ are compared with the true DoA θ while the remaining angles of $\hat{\theta}$ are completely ignored.

The separate classifier is trained using the categorical cross entropy of the classes as a loss function ensuring optimal training. In particular, letting λ_u be the input to the MLP classifier when applying DA-MUSIC to \mathbf{X}_u and letting $\hat{D}(\lambda_u)$

be the softmax output of the MLP applied to λ_u (with $\hat{D}_i(\lambda_u)$ being its i^{th} entry), the loss used for training \mathbf{w}_c is given by

$$\mathcal{L}_{\text{CE}}(D_u, \hat{D}(\lambda_u)) = -\log \hat{D}_{D_u}(\lambda_u). \quad (16)$$

It is noted that since (16) is used for training \mathbf{w}_c , then one should block the gradient during backpropagation from passing from the classifier to the EVD, as indicated by the dashed connections in Fig. 5. This ensures that the MLP learns from the eigenvalues themselves and not by influencing and disrupting the GRU. Further, the regressor is completely independent of the classifier, which allows DA-MUSIC to operate with different classifiers if needed or with any other desired scheme delivering an estimate of D . The resulting training procedure (employing mini-batch gradient descent with ADAM [47]) is summarized as Algorithm 1.

Algorithm 1: Training DA-MUSIC

Data: Data set $\{(\mathbf{X}_u, \theta_u)\}_{u=1}^U$, learning rate $\mu = 0.001$, decay rates $b_1 = 0.9, b_2 = 0.999, \epsilon = 10^{-8}$

- 1 Initialize weights $\mathbf{w}_d, \mathbf{w}_c$;
- 2 Initialize moment vectors $\nu_d, \nu_c, \nu_c, \nu_c$;
- 3 **for** epoch = 1, 2, ... **do**
- 4 **for** each batch **do**
- 5 Apply DA-MUSIC to $\{\mathbf{X}_u\}$ for $u \in \text{batch}$;
- 6 Compute gradients \mathbf{g}_d via
 $\mathbf{g}_d \leftarrow \nabla_{\mathbf{w}_d} \sum_{u \in \text{batch}} \mathcal{L}_{\text{RMSPE}}(\theta_u, \hat{\theta}(\mathbf{X}_u));$
- 7 Compute gradients \mathbf{g}_c via
 $\mathbf{g}_c \leftarrow \nabla_{\mathbf{w}_c} \sum_{u \in \text{batch}} \mathcal{L}_{\text{CE}}(D_u, \hat{D}(\lambda_u));$
- 8 Update biased first moment via
 $\nu_d \leftarrow b_1 \nu_d + (1 - b_1) \mathbf{g}_d;$
- 9 $\nu_c \leftarrow b_1 \nu_c + (1 - b_1) \mathbf{g}_c;$
- 10 Update biased second raw moment via
 $\nu_d \leftarrow b_2 \nu_d + (1 - b_2) \mathbf{g}_d^2;$
- 11 $\nu_c \leftarrow b_2 \nu_c + (1 - b_2) \mathbf{g}_c^2;$
- 12 Compute bias corrected moments $\hat{\nu}_d, \hat{\nu}_c, \hat{\nu}_d, \hat{\nu}_c$;
- 13 Update \mathbf{w}_d via $\mathbf{w}_d \leftarrow \mathbf{w}_d - \mu \hat{\nu}_d / (\sqrt{\hat{\nu}_d} + \epsilon);$
- 14 Update \mathbf{w}_c via $\mathbf{w}_c \leftarrow \mathbf{w}_c - \mu \hat{\nu}_c / (\sqrt{\hat{\nu}_c} + \epsilon);$
- 15 end
- 16 end
- 17 end
- 18 **end**

C. Discussion

The design of the architecture of DA-MUSIC is derived from the model-based MUSIC structure. This allows to exploit the successful aspects of the algorithm while improving certain critical elements and alleviating important drawbacks. Replacing the empirical covariance estimation with a RNN is the key neural augmentation of DA-MUSIC, enabling the system to learn the pseudo covariance from the measurements themselves such that the resulting surrogate model facilitates subspace-based DoA recovery. Thereby, the performance of DA-MUSIC, for example, is not affected by coherent signals and other related issues discussed in Subsection II-D. Furthermore, learning end-to-end allows DA-MUSIC to operate with broadband signals, as it effectively learns to produce a focused pseudo covariance, similarly to the CSS methods discussed in Subsection II-C. It is noted that our augmentation approach depends on the array geometry, as the steering vectors $\mathbf{a}(\cdot)$ are used for computing the MUSIC spectrum. Nonetheless, as we numerically demonstrate in Section IV, DA-MUSIC learns

TABLE I: Simulation parameters.

Parameter Description	Notation	Default Value
Array geometry		ULA
Number of array elements	M	8
Element spacing	Δm	$\ell_{\min}/2$
SNR		10 dB
Snapshots	T	200
Grid points of continuum	R	360
Min. frequency	f_{\min}	0 [Hz]
Max. frequency	f_{\max}	999 [Hz]
Sampling frequency	f_s	$2(f_{\max} + 1)$
Time length	T_{samp}	1 s
FFT points	N_f	$T_{\text{samp}} \cdot f_s$

to overcome mismatches in the array geometry from the data without any alterations or renewed training.

Specifically, the RNN utilized by DA-MUSIC is able to learn an appropriate focusing matrix while concurrently correlating the measurements comparably to (12). The usage of a RNN applied to the time-domain signal and only passing the last state to the next layer allows DA-MUSIC to operate with different signal durations and possibly cope in real-time with dynamic variations in the DoAs, though investigation of the latter is left for future work. Our experiments indicate that a deeper RNN aids the correlation aspect while a wider RNN allows a more complicated mapping with this correlation.

Another important component of the architecture of DA-MUSIC is its incorporation of the EVD as a means for division into subspaces. Though computationally expensive, the internal EVD allows DA-MUSIC to not only classify signal and noise subspaces with the eigenvalues, but also significantly simplifies the estimation of the number of signal sources present.

To enable training end-to-end from the errors in (14), a NN-based peak finder is used in form of a MLP. Model-based peak-finding is generally non-differentiable; therefore, replacing it with a NN enables gradient-based optimization through the entire DA-MUSIC structure. Furthermore, improved resolution can be achieved by extracting the DoA from the spatial spectrum in a learned manner (i.e., $\hat{\theta}_d \in [0, 2\pi)$ and it is not dependent on the number of angles ψ used to evaluate the spectrum $P(\psi)$).

IV. NUMERICAL EVALUATIONS

In this section we present our numerical evaluations of the proposed DA-MUSIC algorithm¹. Our experimental study is comprised of evaluations in a narrowband synthetic setting (Subsection IV-A); a broad synthetic setup (Subsection IV-B); and experiments with real-world data corresponding to azimuth estimation in seismic arrays (Subsection IV-C).

A. Synthetic Narrowband

The numerical evaluations of synthetic data presented below are obtained by simulating the measurements $\mathbf{x}(t)$ according to the narrowband system model (1). In particular, we simulate a ULA with $M = 8$ array elements that measure impinging

¹The source code used in our experiments can be found at <https://github.com/DA-MUSIC/TSP22>.

TABLE II: RMSPE of different DoA estimation algorithms with constant and known D for $T = 200$ snapshots.

RMSPE [rad]	DA-MUSIC	Deep-MUSIC	Classic MUSIC	Beam-former	Random
non-coherent					
$D = 2$	0.0117	0.0329	0.0336	0.1415	0.6809
$D = 3$	0.0315	0.1600	0.0841	0.2814	0.6034
$D = 4$	0.0563	0.2656	0.1459	0.3793	0.5421
$D = 5$	0.0751	0.2701	0.2008	0.4335	0.4963
coherent					
$D = 2$	0.0140	0.5781	0.2350	0.1425	0.6854
$D = 3$	0.0407	0.4023	0.4819	0.2957	0.6060
$D = 4$	0.0519	0.2915	0.4522	0.3343	0.5407
$D = 5$	0.0658	0.3054	0.4401	0.3974	0.5000

waveforms originating from the DoA angles $\boldsymbol{\theta} = [\theta_1 \dots \theta_D]$, which are separately drawn from the uniform distribution $\mathcal{U}(-\pi/2, \pi/2)$. The signals $\mathbf{s}(t) = [s_1(t) \dots s_D(t)]^\top$ are each drawn randomly from the complex Gaussian distribution $\mathcal{CN}(0, 1)$ for all t modeling random amplitudes and phases. The noises measured at the M array elements $\mathbf{v}(t) = [v_1(t) \dots v_M(t)]^\top$ are also drawn from $\mathcal{CN}(0, 1)$ for all t , followed by appropriate scaling to meet the constant SNR. In the coherent cases, all signals have identical amplitudes and phases, and when not stated otherwise, the simulation parameters are set according to Table I.

1) *Known Number of Sources*: We first evaluate the RMSPE in [rad] achieved when the number of sources D is known in the synthetic narrowband scenario described above. The results, reported in Table II, compare the performance of the following DoA estimators for a different number of sources D :

- The DA-MUSIC architecture is implemented according to Fig. 3 and trained separately for each case D .
- The data-driven DeepMUSIC proposed in [18], while incorporating minor alterations that were necessary to accommodate for the difference in the setup, includes tuning of individual hyperparameters to assure successful training of the CNNs.
- The classic MB MUSIC algorithm, implemented as described in Section II-D, utilizes the external knowledge of D .
- A beamformer is implemented in the conventional manner [8].

The above algorithms are compared with a random guessing of the DoA angles. The results in Table II show that the proposed DA-MUSIC notably outperforms all considered benchmarks, notably surpassing the MB MUSIC algorithm not only for coherent sources, but also for non-coherent ones, which is the scenario for which the MB algorithm is designed.

To compare the resolution of the algorithms, Fig. 7 shows the RMSPE for localizing $D = 2$ non-coherent signals, which are located close together at a $\Delta\theta$ distance from each other. The MB MUSIC algorithm is shown to collapse when the angular difference approaches $\Delta\theta \approx 0.1$ radians, while DA-MUSIC demonstrates a constant low error for all $\Delta\theta$, indicating its improved resolution.

Next, we evaluate DA-MUSIC in the presence of a mismatch in the array geometry. Fig. 8 depicts the RMSPE achieved

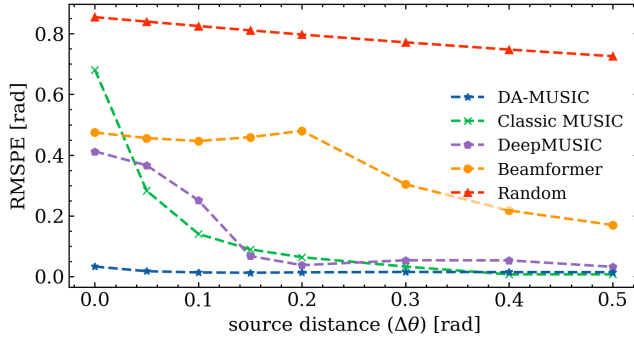


Fig. 7: DoA estimation of $D = 2$ closely spaced sources.

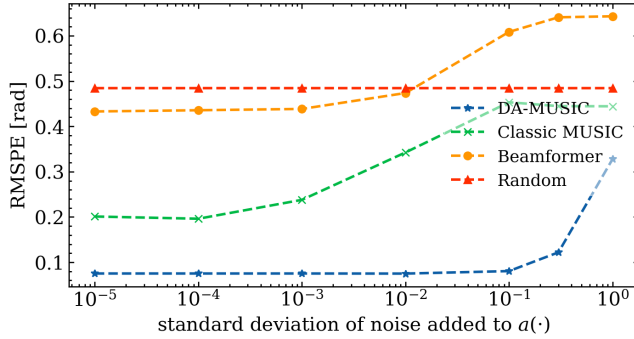


Fig. 8: DoA estimation with mismatch in the array geometry.

when each element of the steering vector $\mathbf{a}(\cdot)$ is corrupted with zero-mean Gaussian noise, leading to a mismatch from the values used to compute the spatial spectrum. Indicating an improved robustness, DA-MUSIC is shown to overcome such mismatches in the array geometry from the data.

We conclude the evaluation of DA-MUSIC with a known number of sources by considering the case in which the SNR is not known during training, and is thus trained using data generated from a mixture of different SNR levels in the range of 0 – 20 dB. Fig.9 depicts the performances differences when localizing $D = 5$ non-coherent signals with various different SNRs. DA-MUSIC shows a constant low SNR even for low settings and without any fluctuations which slowly decreases with increasing SNR.

2) *Unknown and Varying Number of Sources:* Table III shows the results obtained in the exact same narrowband

TABLE III: RMSPE of different DoA estimation algorithms with varying and unknown D for $T = 200$ snapshots.

RMSPE [rad]	DA-MUSIC	Classic MUSIC	Beamformer	Random
non-coherent				
$D = 2$	0.0430	0.0428	0.1900	0.8318
$D = 3$	0.0705	0.0917	0.2906	0.6981
$D = 4$	0.0894	0.1489	0.3757	0.6021
$D = 5$	0.1222	0.1856	0.4029	0.5357
coherent				
$D = 2$	0.0383	0.6139	0.1670	0.8243
$D = 3$	0.0688	0.5743	0.2843	0.6962
$D = 4$	0.0869	0.5258	0.3883	0.6051
$D = 5$	0.1046	0.4744	0.4179	0.5435

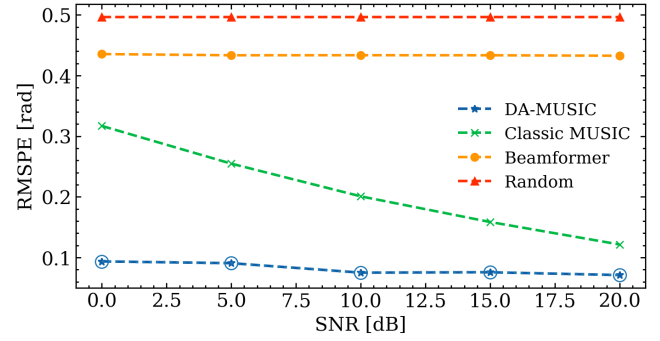


Fig. 9: DoA estimation of $D = 5$ signals with different SNRs.

scenario introduced in Section IV-A above but with an unknown and varying number of sources $D \in \{2, \dots, 5\}$. Here, during inference the DoA estimation algorithms do not have any knowledge of the varying number of sources present. The compute the RMSPE in such settings, if the DoA estimators output the wrong number of sources \hat{D} , the DoA are either truncated (least dominant peaks for the MB algorithms and highest indexed DoA angles for DA-MUSIC) or padded with random DoA angles until $|\hat{\theta}| = |\theta| = D$. We compare the following DoA estimators:

- The DA-MUSIC architecture is implemented according to Fig. 5 with the classifier which predicts the number of sources being trained along with the overall DoA estimation method.
- The DA-MUSIC (RTC) variation is also implemented according to Fig. 5, yet with a retroactively trained classifier (RTC), i.e., we first train DA-MUSIC for a specific scenario, and then we fix the DoA estimator modules and train only the classification network for alternate scenarios.
- The Classic MUSIC algorithm is implemented as before, but determines the number of sources by estimating the multiplicity of the smallest eigenvalue utilizing a pre-determined threshold.
- The Beamformer is implemented as above, though, it utilizes a peak-finder to estimate the number of sources by determining the number of dominant peaks.
- The Random algorithm corresponds to the base performance when choosing DoA angles at random.

Figs. 10 and 11 show the accuracy in identifying the number of sources versus the number of snapshots T obtained by the mentioned algorithms during the estimation of \hat{D} for non-coherent and coherent signals, respectively. DA-MUSIC is only trained for the case $T = 200$ as indicated by the circle around the $T = 200$ marker, yet manages to operate with shorter sequences during inference due to the recurrent unit. Unfortunately, the performance of the internal classifier of DA-MUSIC is dependent on the number of snapshots, and to be able to maintain a more constant accuracy it must to be trained for each case. Consequently, DA-MUSIC (RTC), which trains its classifier retroactively, requires separate training for each number of snapshots, yet manages to achieve the most accurate predictions.

The corresponding performances in localizing the varying

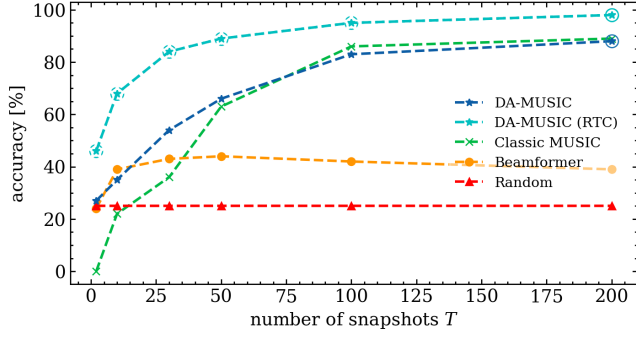


Fig. 10: Accuracy of estimating \hat{D} for various T with $D \in \{2, \dots, 5\}$ non-coherent signals.

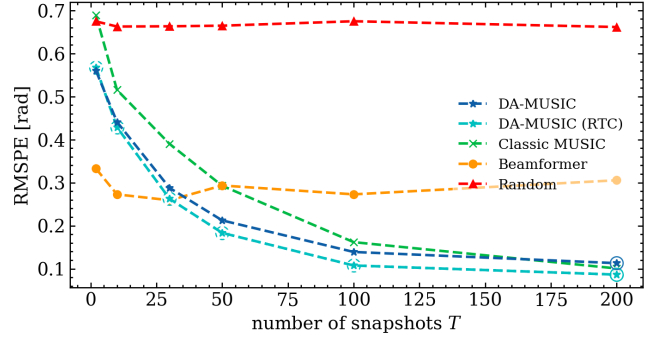


Fig. 12: RMSPE for varying and unknown number of $D \in \{2, \dots, 5\}$ non-coherent signals.

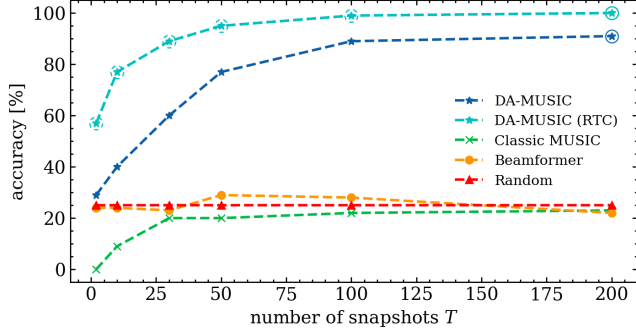


Fig. 11: Accuracy of estimating \hat{D} for various T with $D \in \{2, \dots, 5\}$ coherent signals.

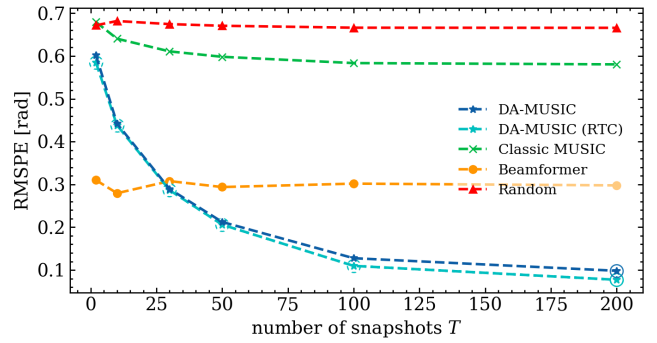


Fig. 13: RMSPE for varying and unknown number of $D \in \{2, \dots, 5\}$ coherent signals.

number of sources are depicted in Figs. 12 and 13 for non-coherent and coherent signals, respectively. The shown RMSPE is an average over all considered $D \in \{2, \dots, 5\}$. The fundamental limitation of the MB MUSIC structure to estimate the number of signal sources for coherent signals also severely impacts the localization abilities of the algorithm. The DA-MUSIC algorithm outperforms the classic MUSIC approach in non-coherent and coherent cases.

B. Synthetic Broadband

We proceed to evaluate DA-MUSIC in a broadband setting. The previously introduced synthetic environment requires certain alterations and assumptions to account for broadband signals. The sensor elements of the receiving array are adequately spaced, and the element spacing is therefore assumed to be

$$\Delta m = \frac{\ell_{\min}}{2} = \frac{1}{2} \frac{c}{f_{\max}}, \quad (17)$$

TABLE IV: Simulation parameters of the broadband scenarios.

	Parameter Description	Notation	Value
Scenario 1	Modulation frequency	$f_{c,d}$	0 – 999 [Hz]
Scenario 2	Number of subcarriers Signal bandwidth	K Δf_d	1000 1000 [Hz]
Scenario 3	Modulation frequency Number of subcarriers Signal bandwidth	$f_{c,d}$ K Δf_d	0 – 899 [Hz] 10 100 [Hz]

where ℓ_{\min} is the minimal wavelength corresponding to the maximal occurring frequency f_{\max} and the frequency spectrum of interest is considered to be within $[f_{\min}, f_{\max}]$. The measurements are simulated utilizing the broadband system model (7), where the elements of $\mathcal{S}(\omega)$ and $\mathcal{W}(\omega)$ are the N_f -point FFTs of the elements of $\mathbf{s}(t)$ and $\mathbf{w}(t)$. The parameter values of the different broadband scenarios are specified in Table IV if not specified otherwise.

We simulate the following DoA estimators:

- The DA-MUSIC architecture is implemented according to Fig. 3, but the GRU parameters are scaled (having 10 times more parameters available) to enable optimal learning despite the more complex broadband scenarios.
- The classic MUSIC algorithm is implemented in its narrowband format as described in Section II-D and utilizes steering vectors calibrated to the exact array element spacing using $\ell_{\min}/2$.
- Broadband MUSIC corresponds to an incoherent broadband extension of MUSIC [35] and is implemented using 10 [Hz] per IFB; i.e., $|\omega_b - \omega_{b-1}| = 10$ [Hz] for all $b \in \{1, \dots, B\}$.
- The DoA estimators are again compared to choosing DoA angles at random.

We consider the following three different signal models of the broadband signals $s_d(t)$ for $d \in \{1, \dots, D\}$:

1) *Broadband Scenario 1*: A broadband signal obtained as narrowband signals modulated on different carrier frequencies,

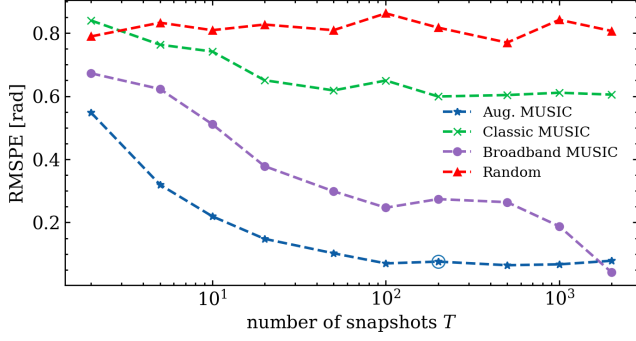


Fig. 14: RMSPE for known number of $D = 2$ signals from Broadband Scenario 1.

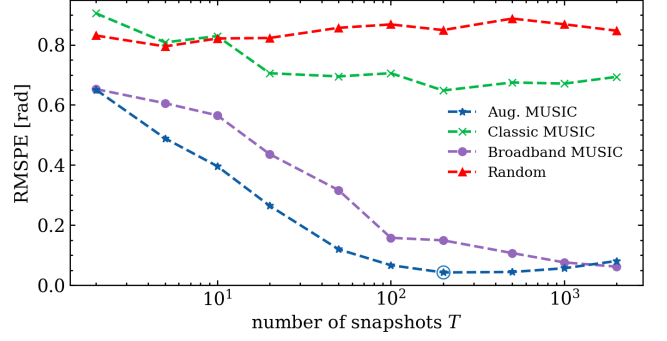


Fig. 16: RMSPE for known number of $D = 2$ signals from Broadband Scenario 3.

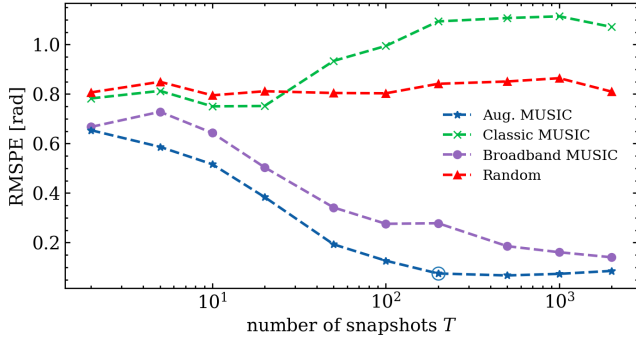


Fig. 15: RMSPE for known number of $D = 2$ signals from Broadband Scenario 2.

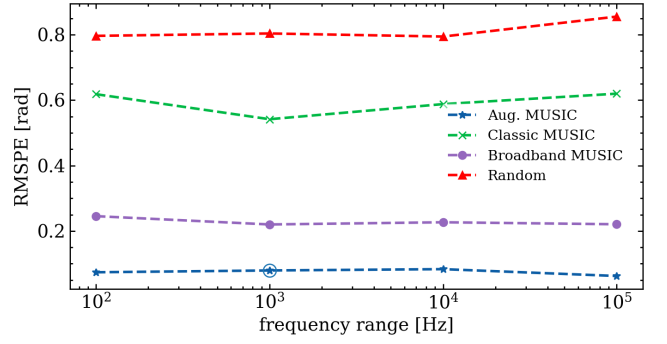


Fig. 17: RMSPE of varying frequency range for the carrier frequencies of Broadband Scenario 1 signals.

i.e.,

$$s_d(t) = \bar{s}_d \exp(2\pi j f_{c,d} t), \quad (18)$$

where for each $d \in \{1, \dots, D\}$, both \bar{s}_d and $f_{c,d}$ are randomly drawn from $\mathcal{CN}(0, 1)$ and $\mathcal{U}(f_{\min}, f_{\max})$ respectively.

2) *Broadband Scenario 2*: Broadband signals obtained via orthogonal frequency division multiplexing (OFDM) [48], which are modulated on the same carrier frequency. The signals are considered in baseband and take the following form

$$s_{d,\text{OFDM}} = \frac{1}{K} \sum_{k=0}^{K-1} \bar{s}_k \exp(2\pi j k \Delta f_d t / K), \quad (19)$$

where $\bar{s}_k \sim \mathcal{CN}(0, 1)$ is randomly drawn for each of the K subcarriers and the bandwidth is $\Delta f_d = f_{\max} - f_{\min}$.

3) *Broadband Scenario 3*: A combination of the two previous scenarios and consists of OFDM signals modulated on different carrier frequencies

$$s_d(t) = \exp(2\pi j f_{c,d} t) s_{d,\text{OFDM}}, \quad (20)$$

where $f_{c,d}$ is drawn randomly from $\mathcal{U}(f_{\min}, f_{\max} - \Delta f_d)$ to account for the signal bandwidth Δf_d .

Results: Figs. 14, 15, and 16 present the RMSPE obtained when localizing $D = 2$ broadband signals from Broadband Scenario 1, 2, and 3 respectively. The number of snapshots goes as high as the sampling frequency $f_s = 2000$ [Hz] and is given logarithmically. This high number is suitable for the MB broadband MUSIC algorithm to achieve reliable transformation from the time domain to the frequency domain. DA-MUSIC

is again only trained for the case $T = 200$, as indicated by a circle around the marker, yet manages to perform similarly well with a higher number of snapshots. As expected, the classic narrowband MUSIC algorithm completely fails to operate with these broadband signals, while DA-MUSIC consistently achieves the most accurate estimates, outperforming the MB broadband MUSIC algorithm, except for Broadband Scenario 3 with a very large number of snapshots $T > 10^3$, where DA-MUSIC trained with much shorter sequences is slightly outperformed by the MB estimator. These results demonstrate the suitability of DA-MUSIC for coping with broadband scenarios with a limited number of observations.

Figs. 17, 18, and 19 analyze the performances with differently sized frequency ranges $[f_{\min}, f_{\max}]$. It is noted that the architecture of DA-MUSIC is almost invariant towards such scalings and manages to handle signals during inference with much larger bandwidths or modulated with higher carrier frequencies than the signals of the training data. Specifically, DA-MUSIC is only trained for signals with carrier frequencies and bandwidths within 0 to 1000 [Hz] as indicated by the circle around the marker. The results in Figs. 17-19 show that DA-MUSIC, whose complexity is fixed, learns to achieve the most accurate estimates, outperforming the MB broadband MUSIC; the latter requires an increase of the number of IFBs to overcome a larger frequency range and has a constant 10 [Hz] per bin in the depicted results leading to a severe increase in computational complexity.

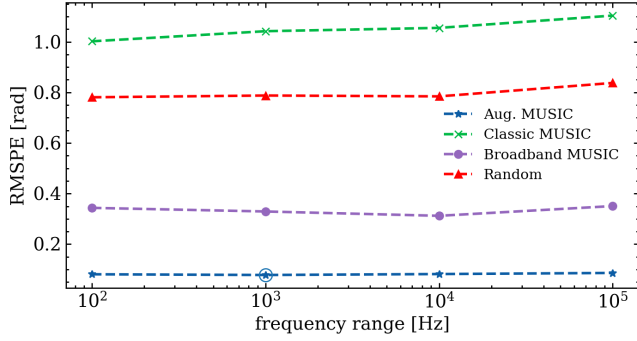


Fig. 18: RMSPE of varying frequency range for the bandwidth of Broadband Scenario 2 signals.

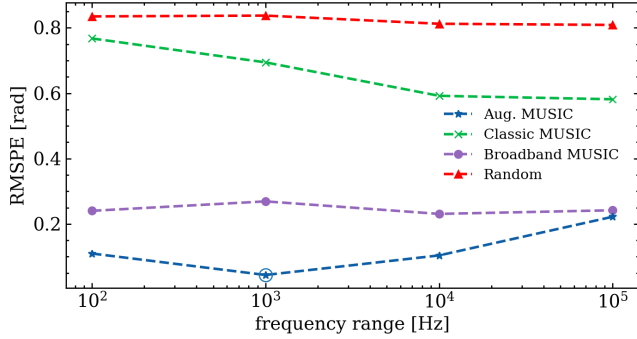


Fig. 19: RMSPE of varying frequency range for the carrier frequencies of Broadband Scenario 3 signals.

C. Non-Synthetic Data: Azimuth Estimation in Seismic Arrays

In this section, we demonstrate the feasibility and the performance of DA-MUSIC in processing non-synthetic seismic data. The seismic data was recorded by the German Experimental Seismic System (GERES) array located in the Bavarian Forest, Germany. GERES is part of the Comprehensive nuclear-Test Ban Treaty Organization (CTBTO) international monitoring system, and is a well maintained and calibrated station. Data from GERES is continuously streamed to the International Data Centre (IDC) of the CTBTO, where it is analyzed. The array is composed of 25 vertical seismometers with a minimal distance between the sites of 124 [m] and an aperture of approximately 2.13 [km]. The seismic signal at each sensor is sampled at 40 [Hz]. Details about the GERES arrays and the exact array configuration can be found in [49].

We use data from October to December 2021, in which GERES detected arrivals for 2904 events of which 2816 were used during this analysis, 2534 for training and 282 for testing. We employ sliding windows of length 100 seconds with a shift of 25 seconds around the signal arrival time as designated by

TABLE V: RMSPE in [rad] of different DoA estimation algorithms for seismic data.

	DA-MUSIC	Broadband MUSIC	Classic MUSIC	Beam-former	Random
RMSPE	0.6269	1.0075	1.2475	0.9383	1.7097

the IDC analysis. The following parameters for each event are obtained from the IDC's Reviewed Event Bulletin: the azimuth DoA angle θ , the slowness value u , and the sensor positions $\mathbf{r}_1, \dots, \mathbf{r}_M$. Using these parameters, the steering vectors take the following form:

$$\mathbf{a}(f, u, \psi, \alpha) = [e^{-j2\pi f u \mathbf{r}_1 \mathbf{k}(\psi, \alpha)} \dots e^{-j2\pi f u \mathbf{r}_M \mathbf{k}(\psi, \alpha)}], \quad (21)$$

for some frequency f and with the wave vector for certain elevation α and azimuth ψ of interest,

$$\mathbf{k}(\psi, \alpha) = [\sin \alpha \cos \psi, \sin \alpha \sin \psi, \cos \alpha]^\top. \quad (22)$$

We compare DA-MUSIC with following DoA estimators for the setting settings $\alpha = -\pi/4$ and $f = 1$ [Hz]:

- Broadband MUSIC, corresponding to an incoherent broadband extension of MUSIC [35], and instead of using the constant $f = 1$ [Hz] it utilizes 10 IFB with frequencies in $[0, 20]$ [Hz].
- The classic MUSIC algorithm, implemented in its narrow-band format as described in Section II-D with additionally filtering the measurements with an experimentally calibrated low-pass filter, allowing only frequencies within $[0, 10]$ [Hz] to pass.
- A conventional beamformer [8].
- Choosing a DoA angle at random.

The results, reported in Table V, show that DA-MUSIC manages to outperform the MB estimators by not only focusing the frequency component, but also by concurrently focusing the interdependent elevation angle to receive a stable azimuth estimation. On the other hand, the MB algorithms require further knowledge of the elevation and frequency at hand to operate reliably. While the errors in Table V may appear to be relatively large, it is noted that the average error achieved via expert analysis reported by the IDC Reviewed Event Bulletin is of 0.4243 [rad]. This indicates on the ability of DA-MUSIC to achieve comparable results and to notably outperform the MB estimators while operating with simplified and approximated model parameters.

V. CONCLUSIONS

We presented a hybrid MB/DD implementation of the MUSIC algorithm for DoA estimation. The proposed deep augmented MUSIC was shown to mitigate some of the limitations and drawbacks of the classic method. DA-MUSIC is operable with an unknown number of sources and with broadband signals, while being adaptable to various scenarios and robust towards severe mismatches in the array geometry. The proposed hybrid MB/DD approach provides a viable alternative in both low and high snapshot domains, and shows a remarkable resolution capability compared to both MB and DD benchmarks in various settings.

VI. ACKNOWLEDGMENT

We thank Dr. Yochai Ben Horin for constructive and valuable joint discussions on the seismic data, and providing the data.

REFERENCES

- [1] J. P. Merkofer, G. Revach, N. Shlezinger, and R. J. G. van Sloun, "Deep augmented music algorithm for data-driven DoA estimation," in *IEEE International Conference on Acoustics, Speech, and Signal Processing (ICASSP)*, 2022, pp. 3598–3602.
- [2] I. Bilik, O. Longman, S. Villeval, and J. Tabrikian, "The rise of radar for autonomous vehicles: Signal processing solutions and future research directions," *IEEE Signal Process. Mag.*, vol. 36, no. 5, pp. 20–31, 2019.
- [3] D. Rahamim, J. Tabrikian, and R. Shavit, "Source localization using vector sensor array in a multipath environment," *IEEE Trans. Signal Process.*, vol. 52, no. 11, pp. 3096–3103, 2004.
- [4] J. Foutz, A. Spanias, and M. K. Banavar, "Narrowband direction of arrival estimation for antenna arrays," *Synthesis Lectures on Antennas*, vol. 3, no. 1, pp. 1–76, 2008.
- [5] H. Krim and M. Viberg, "Two decades of array signal processing research: the parametric approach," *IEEE Signal Process. Mag.*, vol. 13, no. 4, pp. 67–94, 1996.
- [6] Z. Ahmad and I. Ali, "Three decades of development in DoA estimation technology," *Indonesian Journal of Electrical Engineering and Computer Science*, vol. 12, pp. 6297–6312, 2014.
- [7] R. Schmidt, "Multiple emitter location and signal parameter estimation," *IEEE Trans. Antennas Propag.*, vol. 34, no. 3, pp. 276–280, 1986.
- [8] M. S. Bartlett, "Smoothing periodograms from time-series with continuous spectra," *Nature*, vol. 161, no. 4096, pp. 686–687, May 1948.
- [9] J. Capon, "High-resolution frequency-wavenumber spectrum analysis," *Proc. IEEE*, vol. 57, no. 8, pp. 1408–1418, 1969.
- [10] T. E. Tuncer, T. K. Yasar, and B. Friedlander, "Chapter 4 - narrowband and wideband DoA estimation for uniform and nonuniform linear arrays," in *Classical and Modern Direction-of-Arrival Estimation*. Boston: Academic Press, 2009, pp. 125–160.
- [11] H. Wang and M. Kaveh, "Coherent signal-subspace processing for the detection and estimation of angles of arrival of multiple wide-band sources," *IEEE Trans. Acoust., Speech, Signal Process.*, vol. 33, no. 4, pp. 823–831, 1985.
- [12] G. Su and M. Morf, "The signal subspace approach for multiple wide-band emitter location," *IEEE Trans. Acoust., Speech, Signal Process.*, vol. 31, no. 6, pp. 1502–1522, 1983.
- [13] S. Chakrabarty and E. A. Habets, "Multi-speaker DoA estimation using deep convolutional networks trained with noise signals," *IEEE J. Sel. Topics Signal Process.*, vol. 13, no. 1, pp. 8–21, 2019.
- [14] Z.-M. Liu, C. Zhang, and S. Y. Philip, "Direction-of-arrival estimation based on deep neural networks with robustness to array imperfections," *IEEE Trans. Antennas Propag.*, vol. 66, no. 12, pp. 7315–7327, 2018.
- [15] H. Hammer, S. E. Chazan, J. Goldberger, and S. Gannot, "Dynamically localizing multiple speakers based on the time-frequency domain," *EURASIP Journal on Audio, Speech, and Music Processing*, vol. 2021, no. 1, pp. 1–10, 2021.
- [16] N. Shlezinger, J. Whang, Y. C. Eldar, and A. G. Dimakis, "Model-based deep learning," *arXiv preprint arXiv:2012.08405*, 2020.
- [17] N. Shlezinger, Y. C. Eldar, and S. P. Boyd, "Model-based deep learning: On the intersection of deep learning and optimization," *arXiv preprint arXiv:2205.02640*, 2022.
- [18] A. M. Elbir, "DeepMUSIC: Multiple signal classification via deep learning," *IEEE Sensors Letters*, vol. 4, no. 4, pp. 1–4, 2020.
- [19] A. Barthelme and W. Utschick, "DoA estimation using neural network-based covariance matrix reconstruction," *IEEE Signal Process. Lett.*, vol. 28, pp. 783–787, 2021.
- [20] S. Chakrabarty and E. A. Habets, "Broadband DoA estimation using convolutional neural networks trained with noise signals," in *Workshop on Applications of Signal Processing to Audio and Acoustics (WASPAA)*, 2017, pp. 136–140.
- [21] W. Zhu and M. Zhang, "A deep learning architecture for broadband DoA estimation," in *2019 IEEE 19th International Conference on Communication Technology (ICCT)*, 2019, pp. 244–247.
- [22] B. Friedlander, "Chapter 1 - wireless direction-finding fundamentals," in *Classical and Modern Direction-of-Arrival Estimation*, T. E. Tuncer and B. Friedlander, Eds. Boston: Academic Press, 2009, pp. 1–51.
- [23] Z. Chen, G. Gokeda, and Y. Yu, *Introduction to Direction-of-arrival Estimation*. Artech House, 2010.
- [24] S. Ge, K. Li, and S. N. M. Rum, "Deep learning approach in DoA estimation: A systematic literature review," *Mob. Inf. Syst.*, vol. 2021, pp. 6392875:1–6392875:14, 2021.
- [25] O. Frost, "An algorithm for linearly constrained adaptive array processing," *Proc. IEEE*, vol. 60, no. 8, pp. 926–935, 1972.
- [26] B. Van Veen and K. Buckley, "Beamforming: a versatile approach to spatial filtering," *IEEE ASSP Mag.*, vol. 5, no. 2, pp. 4–24, 1988.
- [27] B. Friedlander, "The root-music algorithm for direction finding with interpolated arrays," *Signal Processing*, vol. 30, no. 1, pp. 15–29, 1993.
- [28] Tie-Jun Shan, M. Wax, and T. Kailath, "On spatial smoothing for direction-of-arrival estimation of coherent signals," *IEEE Trans. Acoust., Speech, Signal Process.*, vol. 33, no. 4, pp. 806–811, 1985.
- [29] Qing Chen and Ruolun Liu, "On the explanation of spatial smoothing in music algorithm for coherent sources," in *International Conference on Information Science and Technology*, 2011, pp. 699–702.
- [30] A. Paulraj, R. Roy, and T. Kailath, "Estimation of signal parameters via rotational invariance techniques- esprit," in *Nineteenth Asilomar Conference on Circuits, Systems and Computers*, 1985., 1985, pp. 83–89.
- [31] V. Vasylyshyn, "Direction of arrival estimation using esprit with sparse arrays," in *2009 European Radar Conference (EuRAD)*, 2009, pp. 246–249.
- [32] M. Wax, T.-J. Shan, and T. Kailath, "Spatio-temporal spectral analysis by eigenstructure methods," *IEEE Trans. Acoust., Speech, Signal Process.*, vol. 32, no. 4, pp. 817–827, 1984.
- [33] S. Chandran and M. Ibrahim, "DoA estimation of wide-band signals based on time-frequency analysis," *IEEE J. Ocean. Eng.*, vol. 24, no. 1, pp. 116–121, 1999.
- [34] S. Argentieri and P. Danes, "Broadband variations of the music high-resolution method for sound source localization in robotics," in *2007 IEEE/RSJ International Conference on Intelligent Robots and Systems*, 2007, pp. 2009–2014.
- [35] Y.-S. Yoon, L. M. Kaplan, and J. H. McClellan, "DoA estimation of wideband signals," *Advances in Direction-of-Arrival Estimation*, 2006.
- [36] J. Krolik and D. Swingler, "Focused wide-band array processing by spatial resampling," *IEEE Trans. Acoust., Speech, Signal Process.*, vol. 38, no. 2, pp. 356–360, 1990.
- [37] T.-S. Lee, "Efficient wideband source localization using beamforming invariance technique," *IEEE Trans. Signal Process.*, vol. 42, no. 6, pp. 1376–1387, 1994.
- [38] B. Friedlander and A. Weiss, "Direction finding for wideband signals using an interpolated array," in *Asilomar Conference on Signals, Systems, and Computers*, vol. 1, 1991, pp. 583–587.
- [39] E. di Claudio and R. Parisi, "WAVES: weighted average of signal subspaces for robust wideband direction finding," *IEEE Trans. Signal Process.*, vol. 49, no. 10, pp. 2179–2191, 2001.
- [40] Y.-S. Yoon, L. Kaplan, and J. McClellan, "Tops: new doa estimator for wideband signals," *IEEE Trans. Signal Process.*, vol. 54, no. 6, pp. 1977–1989, 2006.
- [41] F. Ma and X. Zhang, "Wideband doa estimation based on focusing signal subspace," *Signal, Image and Video Processing*, vol. 13, 06 2019.
- [42] S. M. Kay, "Fundamentals of statistical signal processing: estimation theory," *Technometrics*, vol. 37, p. 465, 1993.
- [43] H. Krim and J. Proakis, "Smoothed eigenspace-based parameter estimation," *Automatica*, vol. 30, no. 1, pp. 27–38, 1994, special issue on statistical signal processing and control.
- [44] O. Solomon, R. Cohen, Y. Zhang, Y. Yang, Q. He, J. Luo, R. J. van Sloun, and Y. C. Eldar, "Deep unfolded robust PCA with application to clutter suppression in ultrasound," *IEEE Trans. Med. Imag.*, vol. 39, no. 4, pp. 1051–1063, 2019.
- [45] T. Routtenberg and J. Tabrikian, "Bayesian parameter estimation using periodic cost functions," *IEEE Trans. Signal Process.*, vol. 60, no. 3, pp. 1229–1240, 2011.
- [46] —, "Non-bayesian periodic Cramér-Rao bound," *IEEE Trans. Signal Process.*, vol. 61, no. 4, pp. 1019–1032, 2013.
- [47] D. P. Kingma and J. Ba, "Adam: A method for stochastic optimization," *arXiv preprint arXiv:1412.6980*, 2014.
- [48] S. B. Weinstein, "The history of orthogonal frequency-division multiplexing [history of communications]," *IEEE Commun. Mag.*, vol. 47, no. 11, pp. 26–35, 2009.
- [49] H.-P. Harjes, "Design and siting of a new regional array in central europe," *Bulletin of the Seismological Society of America*, vol. 80, pp. 1801–1817, 1990.